Anal. Bioanal. Electrochem., Vol. 15, No. 2, 2023, 102-117
https://www.doi.org/10.22034/abec.2023.702329

Analytical & Bioanalytical Electrochemistry

Full Paper

Electrochemical Sensor Facilitated by the Synthesis of Cadmium Oxide Nanoparticles Amplified Pre-treated Carbon Paste Electrode for Quantification of Serotonin in the Presence of Epinephrine

Rukaya Banu and B. E. Kumara Swamy*

Department of P.G. Studies and Research in Industrial Chemistry, JnanaSahyadri, Kuvempu University, Shankaraghatta-577 451, Shivamogga, Karnataka, India

*Corresponding Author, Tel.: +918282256228
E-Mail: kumaraswamy21@yahoo.com

Received: 23 December 2022 / Received in revised form: 22 February 2023 / Accepted: 23 February 2023 / Published online: 28 February 2023

Abstract- Herein, the modest co-precipitation mode was implemented to fabricate the cadmium oxide nanoparticles (CdO/NPs). The size, elemental composition and morphological characteristics of the synthesized nanomaterials were confirmed by XRD, EDX and SEM measurements. The designed CdO nanoparticles were exploited for the amplification followed by pre-treatment of carbon paste electrode (CdO/MPCPE) and successfully utilised for the quantification of serotonin (SE) in the presence of epinephrine (EP) at biological pH. The tailored composite sensor proclaims the rapid electron transport behaviour which results in accretion in the oxidation peak signals for SE and EP. The several experimental conditions includes pH of supportive buffer, speed rate and concentration of analytes species were idealised. The CdO/MPCPE displays better sensing capability towards specific and simultaneous quantifications and lower detection limits were achieved. The customised electrode facilitates the high selectivity, excellent electrocatalytic stability, and agreeable results for rapid diagnosis of identical bioactive entities.

Keywords- Carbon paste electrode; Cyclic voltammetry; Differential pulse voltammetry; Electrochemical sensors

1. INTRODUCTION

The current growth and impression of nanoscience and nanotechnology and their applicabilities in the field of analytical chemistry have led to the development of new approaches in the area of biosensing applications. Metal oxide nanoparticles are extensively adopted in the electrochemical sensing of bio-essential materials and matters [1-3]. Nanoparticles flourish special physiological and catalytic functionalities and properties like optimal electronic and optical characteristics, the improved surface area of sensing interaction, excellent ability to promote direct electron transmission between the electrode and the reactive sites of the targeted molecules, biocompatibility, chemical constancy, and enhanced signal responses [4-7]. CdO/NPs are familiar to be an extremely reactive n-type semiconductor and have been exploited in energy storage devices [8], magnetoresistive systems [9], heterogeneous catalysis and other optoelectronic devices [10]. CdO/NPs have beneficial demand due to their supreme electrocatalytic actions towards bio-related compounds such as catecholamine molecules [11].

SE and EP are catecholamine neurochemicals immeasurably crucial for forwarding of neuronal indications between nerve cells in the brain as well as from other regions of the body [12]. SE serves a multifarious range of duties across distinct biological processes, including influencing learning, memory, hunger, happiness, and adjusting the temperature of living. SE ranges that are too low or too high can triggers multiple physical and neurological health challenges such as the scarcity of serotonin thought to perform a character in depression and phobias. The upper ranges of SE bring on serotonin toxicity, restlessness, and confusion [13-17].

EP is a neuromediator and neuroendocrine hormone generated by a small number of neurons in the medulla oblongata and adrenal gland. EP works on a vast array of biological responsibilities and on adrenergic and adrenergic receptors in disparate organs [18-20]. EP acts as a first-line treatment for analphylaxis and is involved in manifold clinical solicitations like heart failure and asthma by relaxing the muscles in the airways and tightening the blood veins. Abnormal EP magnitudes can lead to arrhythmias, pulmonary edema and thyroid hormone deficiency [21,22]. SE and EP are associated with mental status and body functions, their early determination being an important goal for clinical diagnosis.

The carbon component as a working sensor stands out as compared to other electrodes owing to their peerless qualities like low background current, efficacy to incorporate the numerous modifiers while paste designing, involves the simple surface removal regime constancy [21-25]. These electrodes permit scans to larger negative potentials as well as excellent anodic potential windows [26]. This study focuses on the development of an electrochemical sensor facilitated by the modification of prepared CdO/NPs followed by pre-treatment and the designed sensor was employed to concurrent and specific discrimination of SE in the occurrence with EP.

2. EXPERIMENTAL SECTION

2.1. Equipment and Reagents

Electroanalytical experiments were accomplished with the facilitation of CH analyser of model CHI 660c. The electrolytic cell comprised of three electrode pattern includes bare and cadmium oxide modified pre-treated carbon paste (BCPE and CdO/MPCPE) working electrode, saturated calomel reference electrode to measure cell potential and platinum wire counter electrode. The structural analyses, elemental composition and morphological features of the prepared CdO nanoparticles were interpreted by adopting XRD, SEM and EDX approaches.

Analytically pure SE, KCl, $K_4[Fe(CN)_6]$, $Cd(NO_3)_3{\cdot}4H_2O$ and NaOH were brought from Himedia laboratories. EP was gotten from Sigma Aldrich. The silicone oil and pure graphite powder were from Fluka and Merck chemicals. Every solution was freshly procured form doubly demineralised water and the solution of EP was made by employing 0.1 M perchloric acid. Supportive buffer was acquired from Na_2HPO_4 and NaH_2PO_4 in a pH range from 5.8 to 7.8.

2.2. Preparation of CdO nanoparticles

The CdO/NPs were synthesized through co-precipitation practice by dissolving 0.1 M $Cd(NO_3)_3{\cdot}4H_2O$ in 50ml of demineralised water and stirred magnetically for 1 h at room temperature. The precipitating reagent, 1 M NaOH was mixed dropwise to the precursor solution and stirred vigorously until the pH value of the solution reaches 10. The building up of white precipitate was started instantaneously. The mixture was continually stirred for 4 h. Then the formed precipitate was filtered and purified numerous times. The filtered solid was heated at 80 °C for 5 h and the gotten powder was then calcinated at 600 °C for about 3 h.

$$Cd(NO_3)_2{\cdot}4H_2O + NaOH \rightarrow Cd(OH)_2 + 2NaNO_3 + 4H_2O\uparrow$$

$$Cd(OH)_2 \rightarrow CdO + H_2O$$

2.3. Setting up of the working electrodes

The bare carbon paste was framed by blending the admixture of graphite powder and binding paraffin oil (70:30 w/w) in an agate mortar for 30 min to attain the homogeneity of the paste. The paste was then firmly pressed into a cave of the Teflon tube and rubbed using smooth paper to get a shiny crack-free surface and the electrical contact was consummated through copper wire.

The CdO/MCPE was fashioned by plodding the prepared CdO/NPs in varied amounts (2 mg, 4 mg, 6 mg, and 8 mg) with the commixture of mineral oil and graphite powder. The identical blending and stuffing procedures were repeated. Then the amplified CdO/MCPE was

employed towards the study of SE and EP. However, the greater current responsiveness was accomplished at 6mg (Figure 1B) hence it was chosen for electrode amplification. The designed CdO/MCPE was electrochemically pre-treated in order to enhance the electrocatalytic sensitivity of the sensor. The pre-treatment of the sensor was done by the continual sweeping of the potential between -0.4V to 1.2V in being of 0.1M NaOH along the speed rate of 0.05 V/s (Figure 1A). Afterward, the tailored electrode was designated as CdO/MPCPE and employed for electrochemical analysis of SE in the presence of EP.

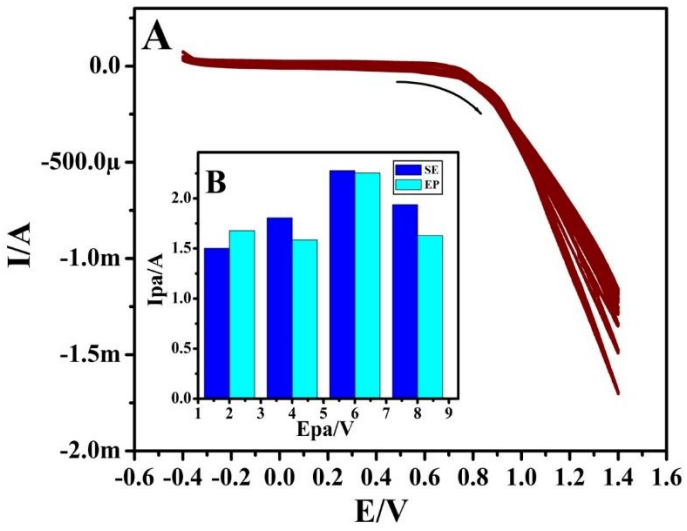

Figure 1. A) Electrochemical pre-treatment of CdO/MCPE in 0.1 M NaOH with the sweep rate 0.05 V/s; B) Plot of I_{pa} of SE and EP versus the amount of synthesised CdO/NPs

3. RESULTS AND DISCUSSION

3.1. Characterisation of synthesised CdO/NPs

The crystalline nature and structure of the as-prepared CdO/NPs were scrutinised by XRD interpretations. Figure 2A displays the XRD patterns of CdO/NPs. The typical diffraction peaks indexed that cubic structure and the reference pattern closely matches with the JCPDS file No. 05-0640. The enhancement in the peak sharpness and nonappearance of the impurity peaks are attributed to the purity and crystallinity of the NPs. The prominent intensive peaks have been employed to estimate the size of the particles through Debye-Scherer formulae (1) [27] and the average grain size was found to be 35 nm.

$$D = \frac{K}{\beta Cos\theta} \quad \text{..... (1)}$$

Where, β is the full width half maximum intensity, θ is the diffraction angle (in radian) of the considered diffraction peak, λ is the wavelength (λ = 0.1543 nm) and K is a constant (0.90). The superficial surface specificities of the prepared CdO/NPs were examined using SEM measurements. Figure 2B depicts the SEM pictures of CdO/NPs. The images clearly evidenced

that the synthesized CdO/NPs have agglomerated structures in which the particles are irregularly fashioned. Figure 2C significantly stipulates the EDX exploration and the emergence of well-defined signals approved the presence of elements, cadmium and oxygen in the as-prepared CdO/NPs.

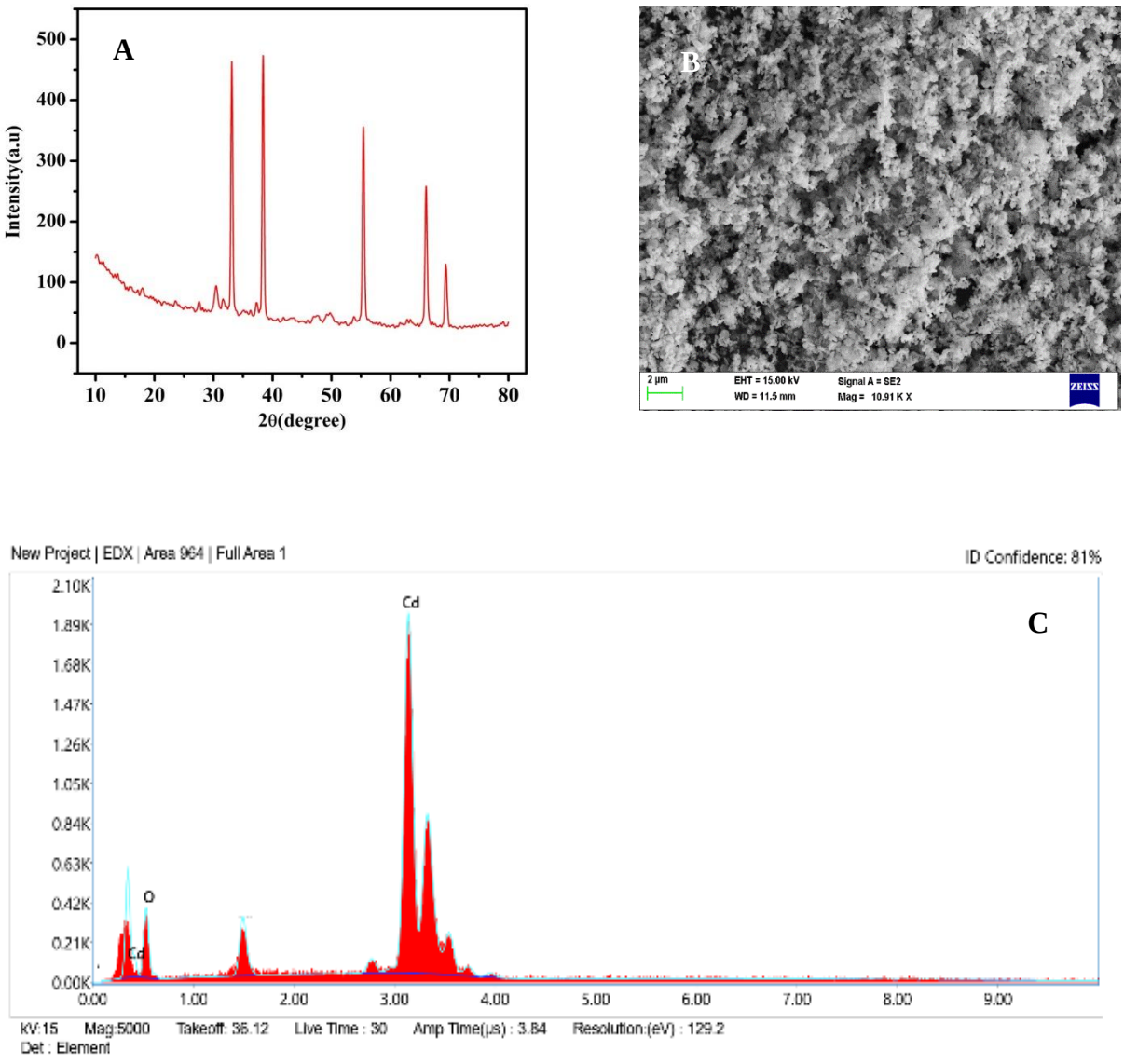

Figure 2. A) XRD pattern for prepared CdO/NPs; B) SEM image of CdO/NPs; C) EDX pattern for as-prepared CdO/NPs

3.2. Electrochemical depiction of CdO/MPCPE

The electron transfer approaches of CdO/MPCPE were monitored by the application of a conventional redox probe ($K_4[Fe(CN)_6]$). Figure 3 presents the CVs developed for the 1 mM $K_4[Fe(CN)_6]$ in bearing with a supporting solution of 1 M KCl having the speed rate of 0.05 V/s at BCPE (dashed curve), CdO/MCPE (dashed-dotted curve) and CdO/MPCPE (solid

curve). The BCPE offered reduced current signals with wider overvoltage and a trifling increment of peak intensity was observed at CdO/MCPE. The substantial hike in the peak current with the lessening of peak potential was perceived at the composite CdO/MPCPE sensor. This outcome testifies that the magnified surface and redox properties along with the rapidity in electron transportation after pre-treatment of the electrode. The availability of effective surface area of the series of working electrodes was enumerated via Randles-Sevick's prescriptions (2) [28]. The composite CdO/MPCPE gave a higher electroactive area (0.0358 cm^2) in contrast to BCPE (0.024 cm^2) and CdO/MCPE (0.0281 cm^2).

$$I_p = (2.69\times10^5)\, n^{3/2}\, A\, D_0^{1/2}\, C_0\, \nu^{1/2} \quad \text{..... (2)}$$

Where, A is the area (cm^2) of the working electrode, C_0 is the concentration (mol/cm^3) of the electroactive substance, ν is the sweep rate and D_0 is the diffusion coefficient (cm^2s^{-1}).

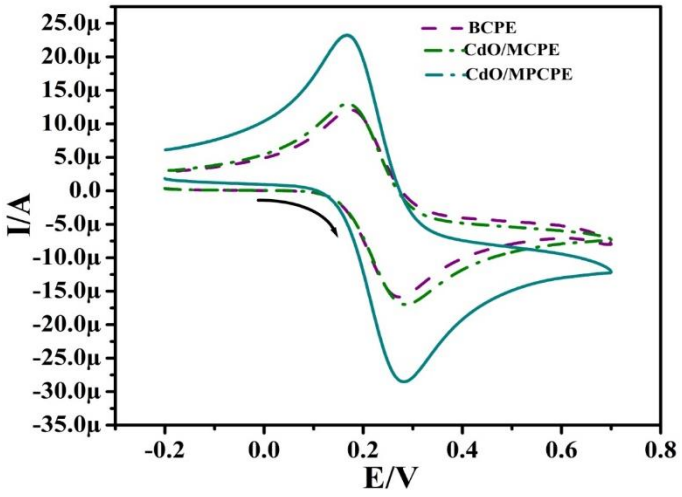

Figure 3. CVs curve for 1 mM $K_4[Fe(CN)_6]$ at BCPE (dashed line), CdO/MCPE(dashed-dotted line), and CdO/MPCPE (solid line) with a sweep rate of 0.05 V/s using 1 M KCl (supporting electrolyte)

3.3. Consequences of solution pH

The optimization of the pH of the supportive medium was found to have influential consequences on the detection sensibility and peak resolution of respective electroactive species. The CV method was accustomed to study the interrelation of the oxidation of SE and EP on pH. Figure 4A and Figure 5A present the CVs logged separately for the 10 µM SE and 10 µM EP at varied pH values (5.8 to 7.8) being with 0.2 M PBS supporting solution at CdO/MPCPE along with 0.05V/s sweep rate. The peak potential moved to the less positive side with increasing buffer pH. This implies the electro-oxidation of SE and EP was governed by protons and electrons. Figure 4B and Figure 5B presents the correlation between peak potential and differed buffer pH and the respective regression equations, E_{pa} (pH 5.8-7.8) = −0.0678 pH+ 0.7963(r^2=0.9912) for SE and E_{pa} (pH 5.8-7.8) = −0.0778 pH+ 0.8963(r^2=0.9895)

for EP respectively. The respective slope value with good linearity confirms the equal number of electron and proton participation [29]. However, the greater peak resolution and sensitivity for SE and EP were witnessed at pH 7.4. So, this pH was elected as optimal for the entire electroanalysis.

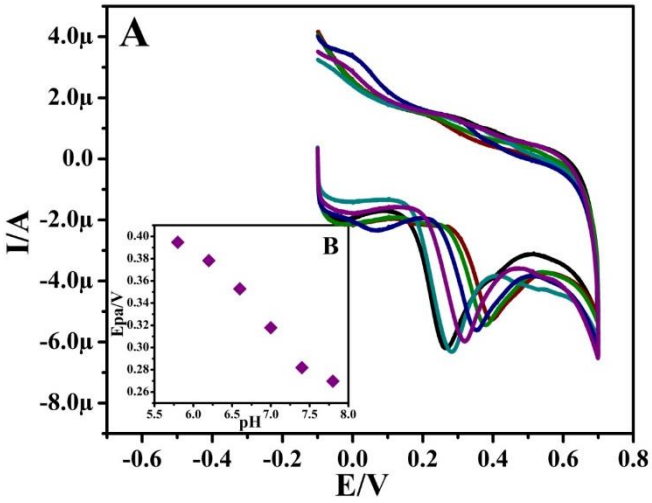

Figure 4. A) CVs curve of 10 µM SE at CdO/MPCPE in the presence of varied pH (5.8 to 7.8) with sweep rate 0.05 V/s; B) Graph of E_{pa} of SE versus pH

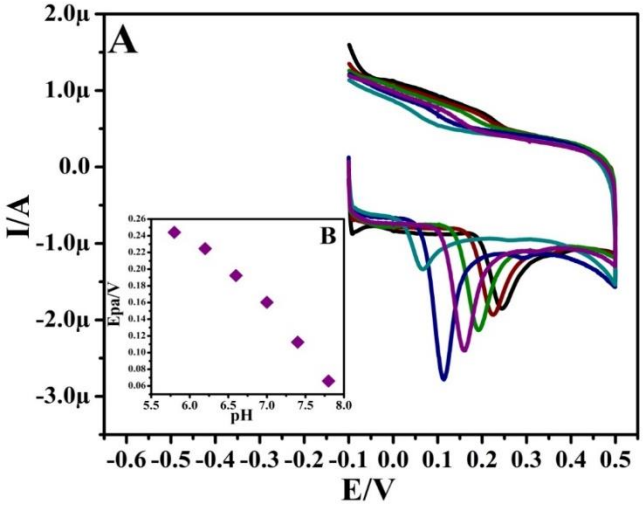

Figure 5. A) CVs curve of 10 µM EP at CdO/MPCPE in the presence of varied pH (5.8 to 7.8) with sweep rate 0.05 V/s; B) Graph of Epa of EP versus pH

3.4. Sensing of SE and EP at the different working electrode

The comparative analytical response of SE and EP were appraised by the CV process to monitor the electrocatalytic implementation of bare and chemically modified working electrodes. The oxidation signals were recorded for 10 µM SE and 10 µM EP at the surface of BCPE (dashed line), CdO/MCPE (dashed-dotted line), and CdO/MPCPE (solid line) in

appearance with 0.2 M PBS of pH 7.4 together with 0.05 V/s scan rate as revealed in Figure 6 and Figure 7 respectively. Contrasted with BCPE, CdO/MCPE displays the minute increment in the anodic peak current. Whereas, after pre-treatment of CdO/MCPE with NaOH, the astronomical hike in the current densities were ascertained with minimisation of over potential. This favourable result authenticates the uplifted surface behaviours, easy electron transfer and higher conductive nature of the composite sensor which makes it as an appropriate choice for the formulation of susceptible SE and EP sensing elements.

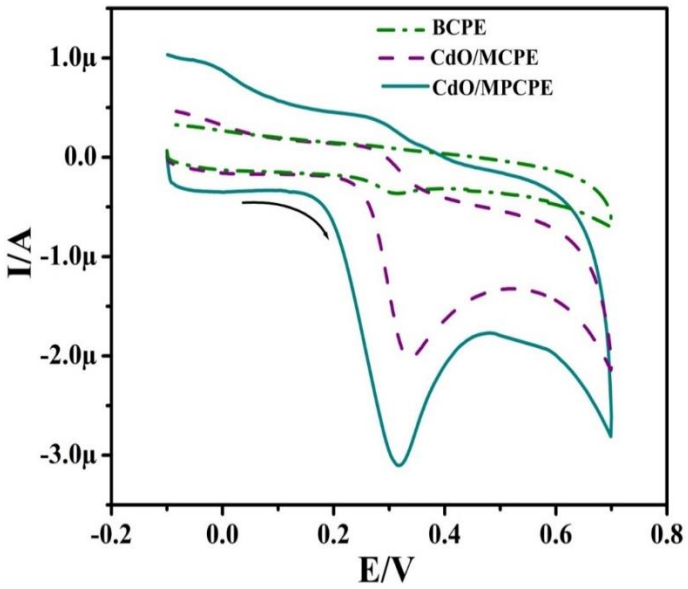

Figure 6. CVs curve for 10 µM SE at BCPE (dashed-dotted line), CdO/MCPE (dashed line), and CdO/MPCPE (solid line) in 0.2 M PBS of pH 7.4 with sweep rate 0.05 V/s

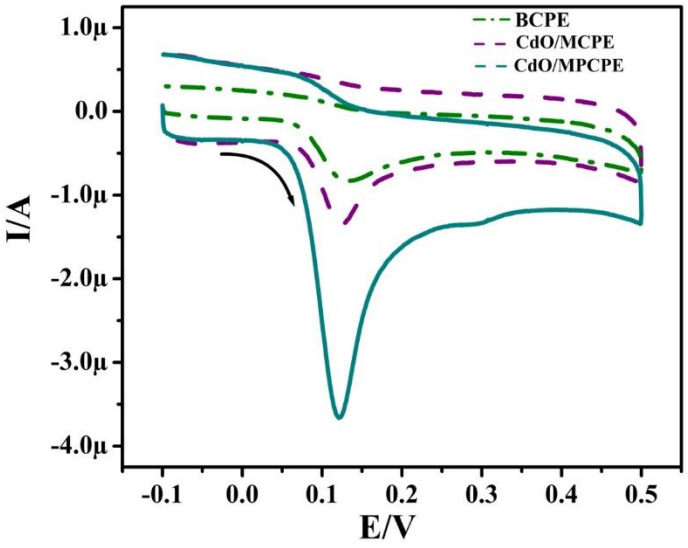

Figure 7. CVs curve for 10 µM EP at BCPE (dashed-dotted line), CdO-MCPE (dashed line), and CdO-MPCPE (solid line) in 0.2 M PBS of pH 7.4 with sweep rate 0.05 V/s

3.5. Study of potential scan rate

The kinetic particularities and oxidation mechanisms were explored for SE and EP at CdO/MPCPE by conducting the study of scan rate variation. CVs registered for 10 µM SE and 10 µM EP in existence with 0.2 M PBS of pH 7.4 with the discrete sweep rate ranging from 0.05 V/s to 0.5 V/s at CdO/MPCPE are provided in Figure 8A and Figure 9A.

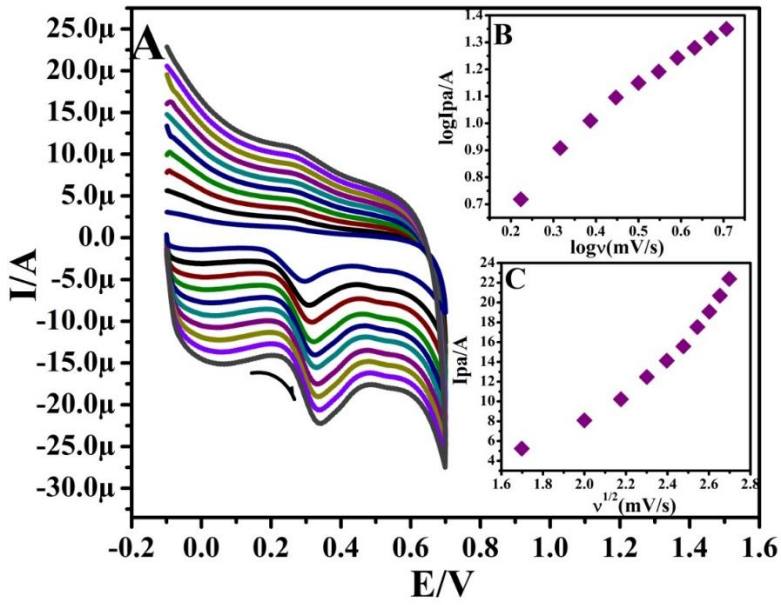

Figure 8. A) CVs curve for 10 µM SE at CdO/MPCPE with varied sweep rates (0.05-0.5 V/s) using 0.2 M PBS of pH 7.4; B) Graph of log I_{pa} versus log of sweep rate; C) Graph of I_{pa} versus square root of sweep rate

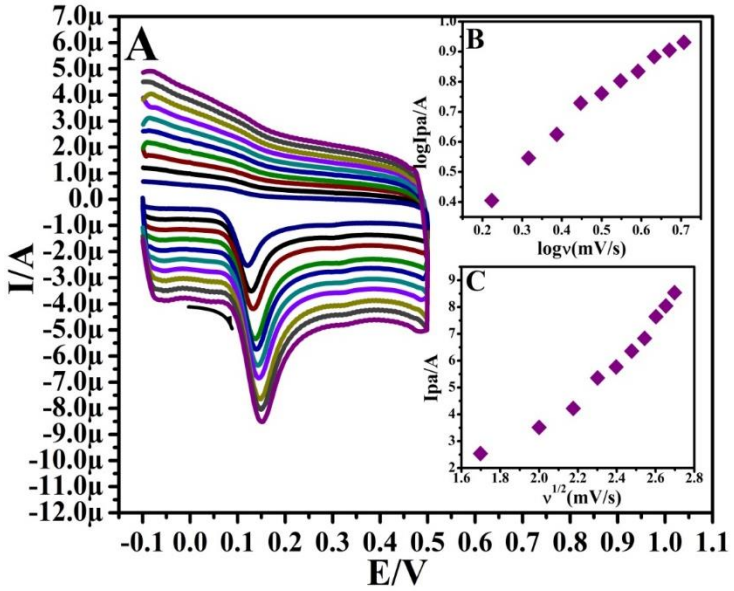

Figure 9. A) CVs curve for 10 µM EP at CdO/MPCPE with varied sweep rates (0.05-0.5 V/s) using 0.2 M PBS of pH 7.4; B) Graph of log I_{pa} versus log of sweep rate; C) Graph of I_{pa} versus square root of sweep rate

As perceived from the figures, the anodic current signals were eventually intensified for a hike in each sweep rate with a positive alteration of peak potential. To assess the electrode kinetics, the graph was plotted between the log I_{pa} of SE and EP against log ν as illustrated in Figures 8B and 9B. The attained graph shows appreciable linearity with the slope values of 1.241 (r^2= 0.98827) for SE and 1.063 (r^2= 0.9894) for EP. This finding affirms that the electrode proceedings were governed by adsorption-controlled phenomenon for both SE and EP [30]. Figure 8C and 9C portrays the plots of I_{pa} of SE and EP versus the Square root of the speed rate ($\nu^{1/2}$). The offered plots show marvellous linearity for SE and EP with a correlation factor r^2= 0.9841 and r^2= 0.9877 respectively, which further accredits the kinetics of the formulated electrode.

3.6. Calibration of CdO/MPCPE towards SE and EP

Under the appropriate test conditions, the sensing efficacy and linear range for the desired analytes were investigated at the surface of the amplified sensor by oscillating the corresponding analyte concentration. CV peaks entered for SE and EP being with 0.2 M PBS of pH 7.4 along with the speed rate 0.05V/s for unfamiliar concentration at CdO/MPCPE using CV technique as indicated in Figure 10A and 11A respectively.

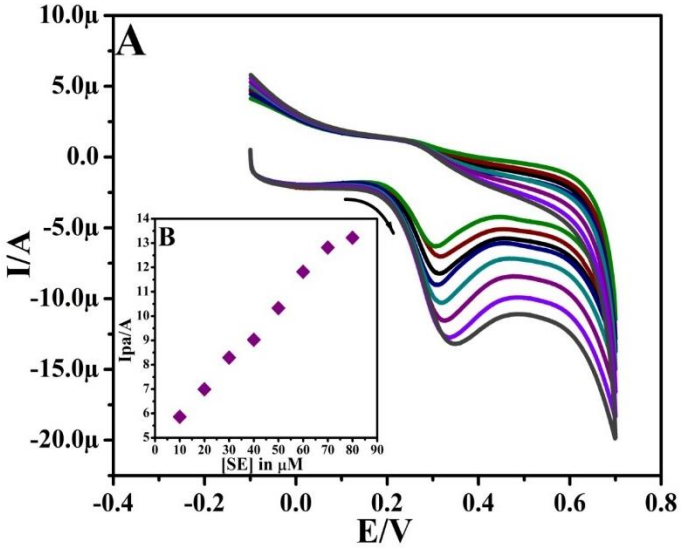

Figure 10. A) CVs curve for SE at CdO/MPCPE with varied concentrations (10-80 µM) using 0.2 M PBS (pH 7.4) with a sweep rate of 0.05 V/s; B) Graph of I_{pa} versus concentration of SE

The gathered outcomes evidenced for that the progressive hike in current signals with boosting the concentration of SE (10 µM-80 µM) and EP (10 µM-100 µM) with diminutive switching of positive peak potential. The calibration graph was plotted for the anodic peak current of SE and EP contrary to the analyte concentration as given in Figures 10B and 11B respectively. The depicted plots reflect the straight line with the correlation expressions, I_{pa}

(μA) = 0.1101 (μM) + 4.83 (r^2 = 0.9953) for SE and I_{pa} (μA) = 0.0536(μM) + 2.12 (r^2 = 0.9979) for EP. The LOD values found to be 0.88 μM for SE and 1.82 μM for EP and LOQ were approximated to be 2.95 μM for SE and 6.07 μM for EP in accordance with the following equalities (2) and (3) [31,32].

$$LOD = 3S/M \quad \text{..... (2)}$$

$$LOQ = 10S/M \quad \text{..... (3)}$$

Where, M is the slope of the calibration curve and S is the standard deviation. The customised sensor portrays the diminished LOD values than many other published electrodes as exposited in Table 1 and Table 2.

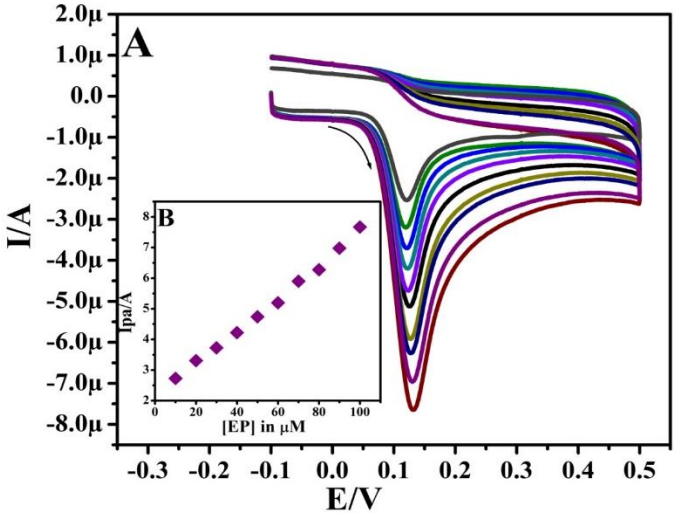

Figure 11. A) CVs curve for EP at CdO/MPCPE with varied concentrations (10-80 μM) using 0.2 M PBS (pH 7.4) with a sweep rate of 0.05 V/s; B) Graph of I_{pa} versus concentration of SE

Table 1. Comparison of the analytical performance of different modified electrodes for SE detection

SI No	Electrode	Detection limit(μM)	Linear range(μM)	Method	Reference
01	AuNPs@PPy/GSPE	3.32	0.1-15	SWV	[33]
02	CDP-Choline/MCPE	5.81	10-100	CV	[34]
03	3D-ITO	7.5	50-1000	DPV	[35]
04	IL-DC-CNT/GE	2.0	5.0-900	DPV	[36]
05	P-VBB/MCPE	0.89	10-70	CV	[30]
06	CdO/MPCPE	0.88	10-80	CV	Present study

Table 2. Comparison of the analytical performance of different modified electrodes for EP detection

SI No	Electrode	Detection limit(μM)	Linear range(μM)	Method	Reference
01	Au 4MpyAuNPs	4.5	10-60	CV	[37]
02	Gold film electrode	19	50-500	CV	[38]
03	TiO_2/MCPE	4.2	1-100	CV	[39]
04	TiO_2/RGO-MCPE	2.0	5-2000	DPV	[40]
05	CAP/MWCNT/GCE	7.2	50-1150	CV	[41]
06	MoS_2-MWCNTs	3.0	9.9-137.9	CV	[42]
07	Cu-ZnO/TX-100/MCPE	3.9	10-80	CV	[43]
08	CdO/MPCPE	1.82	10-100	CV	Present study

3.7. Concurrent electroanalysis of SE and EP at CdO/MPCPE

The competencies to consider the specificities and sensitivity of the customised electrode is its ability to resolve the electroanalytical response of SE in concurred with probable interfering neurochemical like EP. CV method was employed to measure the selectiveness of the modified sensor.

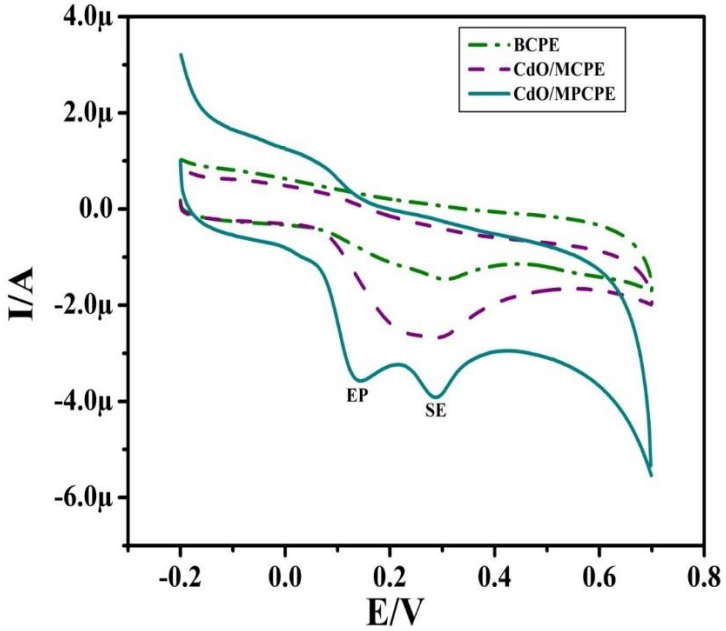

Figure 12. CVs for concurrent detection of SE and EP (10 μM) at BCPE (dashed line) CdO/MCPE (dashed line), and CdO/MPCPE (solid line) in 0.2 M PBS of pH 7.4 with sweep rate 0.05 V/s

Figure 12 displays the CVs documented for a mixed solution of 10μM SE and 10 μM EP in bearing with 0.2 M PBS of pH 7.4 having the scan rate of 0.05 V/s at BCPE (dashed-dotted curve), CdO/MCPE (dashed curve) and CdO/MPCPE (solid curve). The figures depicted that the BCPE and CdO/MCPE was produced less sensitive and failed to resolve the peak potentials of the separate analytes. Whereas, the formulated CdO/MPCPE consequently resolute and distinctly separated peaks of SE and EP were established. The individual peak potential for SE and EP were sited at 0.285 V and 0.1413 V respectively. This outcome signifies the potentiality of the CdO/MPCPE sensor for concurrent and specific discrimination in a mixture of analytes.

3.8. Selective examination of SE and EP at CdO/MPCPE

The isolation of voltammetric signals of the specific analyte in the sample mixture is a key factor to decide the sufficiency of the tailored sensor. The immensely responsive DPV approach was employed to explore the selectivity of SE and EP by differing concentrations and holding the constant concentration of others. DPV response tracked for the SE in the linear range of 10 μM-80 μM by keeping the invariable EP (10 μM) concentration in assistance with 0.2 M PBS of biological pH at CdO/MPCPE as shown in Figure 13A.

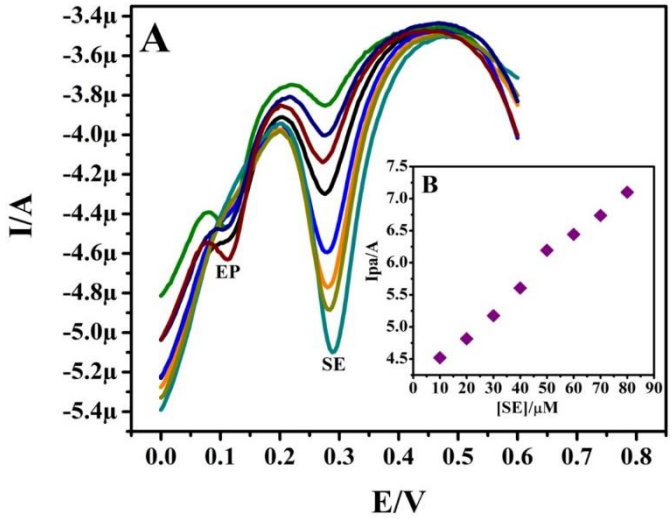

Figure 13. A) DPVs got for varied concentrations of SE (10-80 μM) with EP (10 μM) at CdO/MPCPE with a speed rate of 0.05 V/s in 0.2 M PBS of pH 7.4; B) Display of I_{pa} of SE against concentration

As noticed, the signal density of SE elevated with the rise in its concentration. Identically, to examine the EP, the SE (10 μM) concentration was fixed and the concentration of EP was altered in the range of 10 μM-80 μM as resembled in Figure 14A. Figure 13B and Figure 14B reflect the linearity plot between the I_{pa} of SE and EP with fluctuated concentration. It can be notable from the above outcome; the oxidation peak currents of SE and EP are positively

proportional to their concentration and changing the concentration of one species does not affect the peak current and peak potential of another species. It signifies the greater selectivity of the formulated sensor.

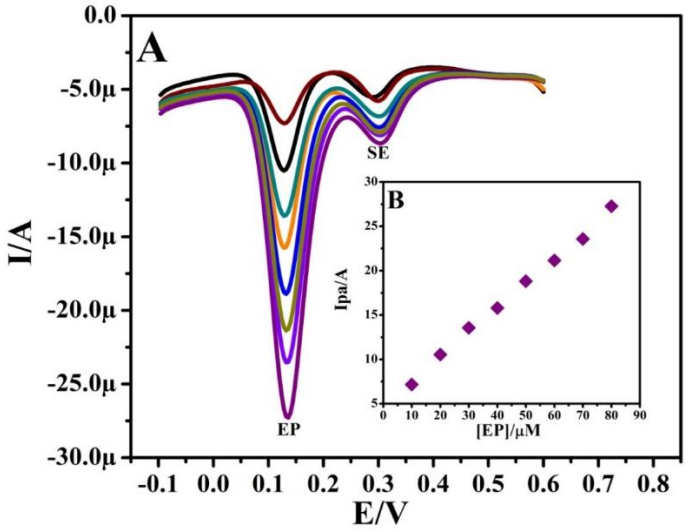

Figure 14. A) DPVs got for varied concentrations of EP (10-80 μM) with SE (10 μM) at CdO/MPCPE with a speed rate of 0.05 V/s in 0.2 M PBS of pH 7.4; B) Display of I_{pa} of EP against concentration

4. CONCLUSION

Herein, the CdO nanoparticles were prepped with the help of chemical co-precipitation fashions and the morphological and other qualities of the developed material was performed using XRD, SEM, and EDX analysis. The electrocatalytic properties were scrutinised by applying the CV and DPV procedures. The as-prepared nanoparticles were utilised for the fabrication of CdO/MCPE and then followed by pre-treatment with NaOH. The customised CdO/MPCPE portrays the augmented voltammetric reactivity and intensified reactive area of the electrode surface towards the identification of SE and EP in physiological pH (7.4). The kinetic experiments were operated to acknowledge the type of electrode process and it was recognised to be adsorption controlled for both SE and EP. The formed CdO/MPCPE electrode yielded lower LOD (0.88 μM for SE and 1.82 μM for EP) and LOQ (2.95 μM for SE and 6.07 μM for EP) values and specific in the isolation of SE from a commixture consisting of both SE and EP with elevation in anodic current. The designed sensor protects the surface of an electrode from fouling and presents favourable sensibility and efficaciously applicable as a biosensor in neurochemistry applications and the quantification of like bioactive elements.

REFERENCES

[1] W. Q. Lim, and Z. Gao, Electroanal. 27 (2015) 1.

[2] J. M. George, A. Antony, and B. Mathew, Microchem. Acta 185 (2018).
[3] S. Sawan, R. Maalouf, A. Errachid, and N. J. Renault, Trends in Anal. Chem. 131 (2020) 116016.
[4] I. Khan, K. Saed, and I. Khan, Arab. J. Chem. 12 (2019) 901.
[5] M. F. Garcia, and J. A. Rodriguez, Nanomaterials, Inorganic and Bioinorganic Perspectives (2017) 11973.
[6] Y. Zhao, X. Ren, F. Zheng, X. Jin, X. Dong, Z. Zhao, and X. Duan, Opto-Electron. Adv. 4 (2021) 200101.
[7] Y. Jiang, W. Zheng, K. Tran, E. Kamilar, J. Bariwal, and H. Liang, Nat. Commun. 13 (2022) 197.
[8] B. Khalilzadeh, M. Hasanzadeh, S. Sanati, L. Saghatforoush, N. Shadjou, J. N. Dolatabadi, and P. Sheikhzadeh, Int. J. Electrochem. Sci. 6 (2011) 4164.
[9] M. Negahdary, S. A. Sadeghi, M. H. Michak, S. R. Zarchi, F. Salahi, N. Mohammadi, E. Azargoon, and A. Sayad, Int. J. Electrochem. Sci. 7 (2012) 6059.
[10] H. Okabe, J. Akimitsu, T. Kubodera, M. Matoba, T. Kyomen,, and M. Itoh, Physica B: Condensed Matter. 378-380 (2006) 863.
[11] S. Cheraghi, M.A. Taher, and H. Karimi-Maleh, Electroanalysis 28 (2016) 366.
[12] S. Ahmadzadeh, F. Karimi, N. Atar, E.R. Sartori, E. Faghih-Mirzaei, and E. Afsharmanesh, Inorg. Nano-Metal Chem. 47 (2017) 347.
[13] S. Reddy, B.E.K. Swamy, U. Chandra, B.S. Sherigara, and H. Jayadevappa, Int. J. Electrochem. Sci. 5 (2010) 10.
[14] P. V. Narayana, T. M. Reddy, P. Gopal, M. M. Reddy, and G. R. Naidu, Mater. Sci. Eng. C 56 (2015) 57.
[15] J. Yeo, and J. Chang, Electrochem. Acta 409 (2022) 139973.
[16] G. Singh, A. Kushwaha, and M. Sharma, Mater. Chem. Phy. 279 (2022) 125782.
[17] R. Rejithamol, R. G. Krishnan, and S. Beena, Mater. Chem. Phy. 258 (2021) 123857.
[18] Y. Dong, and L. Zhang, Sens. Acutarors, B 368 (2022) 132140.
[19] F. Fazl, and M. B. Gholivand, Talanta 239 (2022) 122982.
[20] M. Baniasadi, S. Jahani, H. Maaref and R. Alizadeh, Anal. Bioanal. Electrochem. 9 (2017) 718.
[21] G. E. Uwaya, Y. Wen, and K. Bisetty, J. Electroanal. Chem. 911 (2022) 116204.
[22] S. Kalia, D. S. Rana, N. Thakur, D. Singh, R. Kumar, and R. K. Singh, Mater. Chem. Phy. 287 (2022) 126274.
[23] J.G. Manjunatha, B. E. Kumara Swamy, M. Deraman, and G. P. Mamatha, Der Pharma Chemica 4 (2012) 2489.
[24] N. Hareesha, and J. G. Manjunatha, J. Sci. Adv. Mater. Dev. 5 (2020) 502.
[25] J. G. Manjunatha, B. E. Kumara Swamy, G. P. Mamatha, S. S. Shankar, O. Gilbert, B. N. Chandrashekar, and B. S. Sherigara, Int. J. Electrochem. Sci. 4 (2009) 1469.

[26] N. Hareesha, J. G. Manjunatha, C. Raril, and G. Tigari, Chem. Select. 4 (2019) 4559.
[27] N. Lavanya, E. Fazio, F. Neri, A. Bonavita, S.G. Leonardi, G. Neri, and C. Sekar, Sens. Actuators B 221 (2015) 1412.
[28] N. Hareesha, and J. G. Manjunatha, Mater. Res. Innov. 24 (2026) 349.
[29] J. G. Manjunatha, Chem. Data. Collect. 25 (2020) 100331.
[30] Rukaya Banu, B. E. Kumara Swamy, G. K. Jayaprakash, and S.C. Sharma, Inorg. Chem. Commun. 144 (2022) 109627.
[31] S. S. Shankar, and B. E. K. Swamy, Int. J. Electrochem. Sci. 9 (2014) 1321.
[32] J. K. Shashikumara, B. E. Kumara Swamy, S. C. Sharma, S. A. Hariprasad, and K. Mohanty. Scientific Reports 11 (2021) 14310.
[33] M T A. Cernat, D L A. Florea, D. Bogdan, M. Suciu, R. Sandulescu, and C. Cristea, Electro. Commun. 75 (2017) 43.
[34] S. Deepa, B. E. Kumaraswamy, and K. Vasantakumara Pai, Materials Science for Energy Technologies 3 (2020) 584.
[35] L. Matuschek, G. Gobel, and F. Lisdat, Electrochem. Commun. 81 (2017) 145.
[36] M.M. Ardakani, and A. Khoshroo, J. Electroanal. Chem. 717 (2014) 17.
[37] S. Ramirez, N. Silva, M.P. Oyaizu, J. Pavez, and J.F. Silva, J. Appl. Electrochem. 799 (2017) 349.
[38] M. Dina, A. Fouad, and El-Said Waleed, Journal of Nanomaterials (2016) Article ID 6194230.
[39] K. G. Manjunatha, B. E. K. Swamy, H. D. Madhuchandra, and K. A. Vishnumurthy, Chem. Data. Collect. 31 (2021) 100604.
[40] T. Joseph, and N. Thomas, Mater. Today: Proceedings 41 (2021) 606.
[41] L. V. D. Silva, N. D. D. Santos, A. K. A. de Almeida, D. D. E. R. D. Santos, A. C. F. Santos, M. C. Franca, D. J. P. Lima, P. R. Lima, and M. O. F. Goulat, J. Electroanal. Chem. 881 (2021) 114919
[42] S. Kumar, A. Awasthi, M. D. Sharma, K. Singh, and D. Singh, Mater. Chem. Phy. 290 (2022) 126656.
[43] K. G. Manjunatha, B. E. K. Swamy, G. K. Jayaprakash, S. C. Sharma, P. Lalitha, and K. A. Vishnumurthy, Inorg. Chem. Commun. 142 (2022) 109630.